International Journal of Signal Processing, Image Processing and Pattern Recognition
Vol.9, No.7 (2016), pp.293-304
http://dx.doi.org/10.14257/ijsip.2016.9.7.26

Design and Analysis of Metamaterial Antenna Using Double Square Rings

Tong Huang

XIAN Innovation College of YANAN University
huangtong2008@163.com

Abstract

In this paper, the design and the analysis of the double square ring (DSR) metamaterial is presented, which is based on the equivalent circuit theory and the analysis of the distribution of the electromagnetic field. Based on the retrieval algorithm, the effect of the structural parameters on the effective permittivity and the effective permeability are proposed. The effective permittivity and the effective permeability of the designed DSR metamaterial are simultaneously negative in the range from 4.8GHz to 5.65GHz. A conventional microstrip antenna is designed as comparison, and the analysis of the microstrip antenna is not written in this paper for brevity. The superstrate is composed of an 4×4 *array of the DSR metamaterial, and the novel antenna is consist of the conventional microstrip antenna and the superstrate. The effect of the distance between the superstrate and the antenna are simulated by HFSS software, and the novel antenna is proposed according to the analysis of the distance. The simulation results show that the gain of the novel antenna increased by 1.1dB, and the half power beam width decreased by 40.9°. Therefore, it is concluded that the performance of microstrip antenna can be improved by using DSR metamaterials.*

Keywords*: metamaterial, microstrip antenna, gain, half power beam width*

1. Introduction

In 1968, Veselago proposed the term "metamaterial" refer to the materials with negative effective permittivity and the negative effective permeability [1]. However, the metamaterial did not exist in nature. Even the metamaterial could realize different characteristics from conventional materials, the metamaterial had been ignored for a long time. Until 2000, the interest on the metamaterial was renewed as the two-dimensional array which exhibit negative refractive index was proposed by Pendry [2]. Almost at the same time, the split-ring resonators (SRRs) which obtain the negative effective permittivity were proposed by Shelby. From then on, many researches had been carried out to design metamaterial [3-4]. Smith firstly demonstrated the realization of the metamaterial. The SRRs and wires were placed alternately to achieve the negative effective permittivity and the negative effective permeability simultaneously.

The essential feature of the metamaterial is negative permittivity and negative permeability, while the permittivity and the permeability of the traditional medium are positive [5]. According to the individual Maxwell curl equation of the electric field, the electric field E , the magnetic field H , and the propagation vector k formed "right-handed" (RH) rule in the traditional medium [6]. However, the three vectors formed "left-handed" (LH) rule in the metamaterial. Due to this essential feature of the metamaterial, many fantastic characteristics have been found such as the reversal of Snell's law, reversed Doppler Effect, Vavilov-Cerenkov effect, *etc.* [7-8] .Hence, the metamaterial are termed as "left-handed material" or "negative index material" and so on.

The antenna's micromation is one of the key technologies of communication [8]. The

ISSN: 2005-4254 IJSIP

microstrip patch antennas have advantages such as light weight, low volume, easily integration and so on. While low gain is the major disadvantage of the microstrip patch antenna. Therefore, a method to improve the gain of the microstrip antenna is badly needed.

It has been proved that the metamaterial can improve the performance of the microstrip patch antenna [9-10]. The radome based the regular hexagon metamaterials were placed above the microstrip antenna, and the gain of the antenna improved 2.5dB [11], while the bandwidth of the double negative property is narrow. The distance between patch antenna and metamaterial was analyzed in the literature [12], while the half power beam width (HPBW) were not reduced. It is no doubt that how to further improve the radiation characteristic of the microstrip patch antenna is still the challenge [13].

This article is arranged as follows. Section Ⅱ proposes a double square ring (DSR), and the equivalent circuit of the metamaterial is proposed based the distribution of the electric field and the distribution of the current. The effect of the parameters on the effective permittivity and the effective permeability are analyzed in section Ⅱ as well. Section Ⅲ proposes a conventional microstrip patch antenna with its performance. In section Ⅳ, the effect of the distance between the superstrate and the antenna on the radiation characteristic are analyzed. As a consequence of the analysis of the distance, the novel antenna is designed at last. Finally, a conclusion that the performance of the microstrip patch antenna can be improved by the use of metamaterial is put forward in the section Ⅴ.

2. DSR Design and Analysis

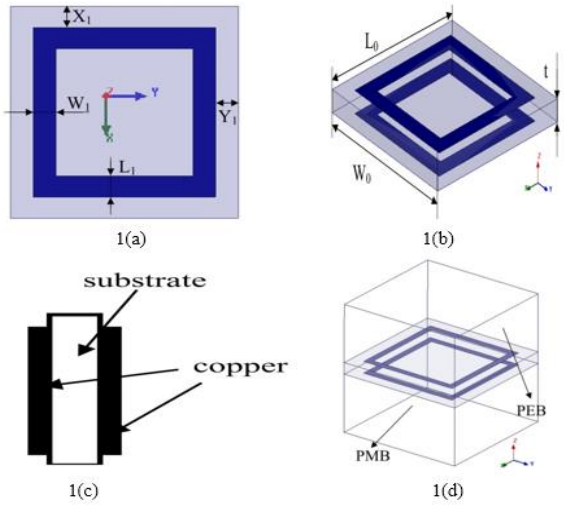

Figure 1. The Schematic of the DSR

(a) front view; (b) angular view; (c) side view; (d) boundary conditions

The DSR structure was proposed in 2012 [14], the Structure diagram is shown in Figure 1 (a) and Figure 1 (b). The metallic rings are made of copper with the thickness of 17μm. The two square rings are located at the top of the substrate and the bottom, as shown in the Figure 1 (c). The relative dielectric constant of the substrate is 4.4 with the Loss tangent is 0.02, the thickness of the substrate is 1mm. The length of the substrate is 10 mm, the width of the substrate is 10mm as well. The width of the square ring is 1 mm, the distance from the square ring to the edge of the dielectric substrate is 1mm.

The simulation of the DSR is carried out using HFSS software. The boundary conditions are set as the reference [14]. The perfect electric boundary condition (PEB) is constructed along the Y axis, and the perfect magnetic boundary condition (PMB) is constructed along the X axis. The wave ports are set in Z axis. The Figure 1 (d) demonstrates the boundary condition of the simulation of the DSR.

In order to have a deeper insight into the mechanism of the magnetic and electric responses, the distribution of the electric field and the magnetic field, and the distribution of the current are carried out. All the distributions of the field are carried out at the resonating frequency.

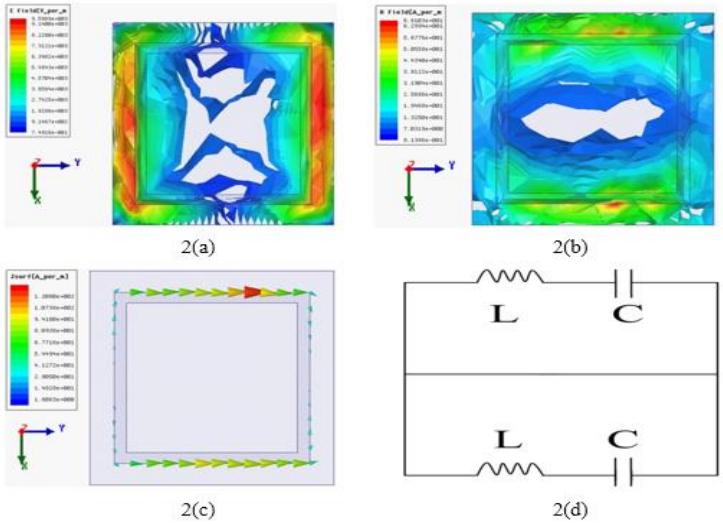

Figure 2. The Distribution of the Fields

(a) electric field; (b) magnetic field; (c) the current; (d) equivalent circuit

The Figure 2 (a) shows the distribution of the electric fields. It can be observed that the electric fields are mainly concentrated in the metallic strips which along the X-axis. It can be deduced that the electric charges are gathered in these strips. Based on the equivalent circuit theory, these metallic strips have the effect of the capacitors.

The Figure 2 (b) illustrates the distribution of the magnetic fields. It can be observed that the magnetic fields are mainly concentrated in the metallic strips which along the Y-axis. These metallic strips have the effect of the inductances based on the equivalent circuit theory.

The distributions of the current are shown in the Figure 2 (c). It shows that the two currents in the same directions and it can be concluded that the two circuits are parallel. As a consequence of the analysis of the distribution of the electric field and the magnetic field, the equivalent circuit of the DSR can be expressed as the Figure 2 (d).

The X-direction metallic strips forms the capacitance C, and the Y- direction metallic strips forms the inductance L. The total capacitance of the circuit is represented as C_t. Based the equivalent circuit, the C_t is

$$C_t = \frac{C}{2} \tag{1}$$

The total inductance of the circuit is represented as L_t. Based the equivalent circuit, the L_t is

$$L_t = 2L \tag{2}$$

The resonance frequency of the DSR is

$$\omega_{m0} = \sqrt{\frac{1}{L_t C_t}} = \sqrt{\frac{1}{LC}} \tag{3}$$

The plasma frequency of the DSR is

$$\omega_{mp} = \frac{1}{\sqrt{1-F}}\omega_{m0} \tag{4}$$

Where the F is the fractional area of the unit cell [15].

The equivalent inductance is represented as [16]

$$L = \mu_0(L_0 - 2X_1 - 2L_1)(W_0 - 2Y_1 - 2W_1) \tag{5}$$

The equivalent capacitance is calculated by [16]

$$C = \frac{\varepsilon_o \varepsilon_r (L_0 - 2X_1)W_1}{t} \tag{6}$$

Therefore, the resonance frequency is

$$\omega_{m0} = \sqrt{\frac{t}{\varepsilon_0 \varepsilon_r (L_0 - 2X_1)W_1 \mu_0 (L_0 - 2X_1 - 2L_1)(W_0 - 2Y_1 - 2W_1)}} \tag{7}$$

Based on the equivalent theory [16], the effective permittivity and the effective permeability of the DSR can be calculated. The widely used retrieval algorithm is [16]

$$n = \frac{1}{kt}\cos^{-1}\left[\frac{1}{2S_{21}}(1 - S_{11}^2 + S_{21}^2)\right] \tag{8}$$

$$z = \sqrt{\frac{(1+S_{11})^2 - S_{21}^2}{(1-S_{11})^2 - S_{21}^2}} \tag{9}$$

$$\varepsilon = n/z \tag{10}$$

$$\mu = nz \tag{11}$$

The S_{11} and the S_{21} represent for the reflection and transmission data, and the wave number of free space represented as the parameter k, the parameter t represents for the thickness of the DSR, n is the refractive index, z is the wave impedance [16].

The relationship between the effective permittivity with the frequency, and the relationship between the effective permeability with the frequency, can be proposed from the retrieval algorithm. In the range $\omega_{m0} < \omega < \omega_{mp}$, the effective permittivity and the effective permeability are negative [17]. The ω_{m0} is the resonance frequency, and the ω_{m0} is the plasma frequency [18]。

Due to the resonance frequency and the plasma frequency depend on the LC resonant circuit, it is no doubt that the parameters of the DSR have an effect on the resonance frequency and the plasma frequency [19]. That is, the parameters have an effect on the frequency band of the negative effective permeability and the frequency band of the negative effective permeability.

The parameter X_1 represents for the X-direction distance between the edge of the metallic strip and the edge of the substrate, and it varied in five steps of 0.2mm each, that is $X_1 = 0.6mm$, $X_1 = 0.8mm$, $X_1 = 1.0mm$, $X_1 = 1.2mm$, $X_1 = 1.4mm$. The effect of the X-direction distance on the effective permittivity and the effective permeability are shown in Figure 3 (a) and Figure 3 (b).

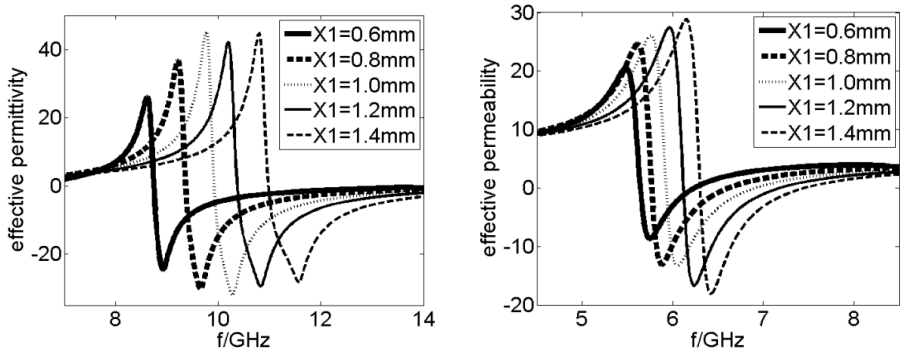

3(a) 3(b)

Figure 3. The Retrieved Parameter Versus Frequency Plot

(a) effective permittivity versus frequency plot; (b) effective permeability versus frequency plot

According to the Figure 3, it can be found that the frequency range of the negative effective permittivity is dependent on the X-direction distance. With the distance increase, the negative frequency band shift from low frequency band to high frequency band, that is the resonance frequency and the plasma frequency increased. The range of the negative effective permeability shares the same regular with the effective permittivity.

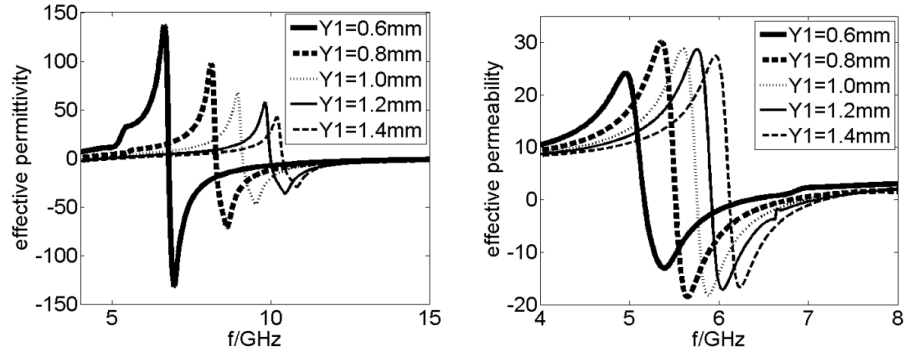

4(a) 4(b)

Figure 4. The Retrieved Parameter Versus Frequency Plot

(a) effective permittivity versus frequency plot; (b) effective permeability versus frequency plot

The parameter Y_1 represents for the Y-direction distance between the edge of the metallic strip and the edge of the substrate, and it varied in five steps of 0.2mm each, that is $Y_1 = 0.6mm$, $Y_1 = 0.8mm$, $Y_1 = 1.0mm$, $Y_1 = 1.2mm$, $Y_1 = 1.4mm$. The effect of the Y-direction distance on the effective permittivity and the effective permeability are shown in Figure 4(a) and Figure 4(b).

It indicates that the effect of Y-direction distance on the effective permittivity and the effect on the effective permeability are similar to the regular of the X-direction distance.

The parameter L_1 represents for the width of the X-direction strip, and it varied in five steps of 0.2mm each, that is $L_1 = 0.6mm$, $L_1 = 0.8mm$, $L_1 = 1.0mm$, $L_1 = 1.2mm$, $L_1 = 1.4mm$ .The effect of the Y-direction distance on the effective permittivity and the effective permeability are shown in Figure 5 (a) and Figure 5 (b).

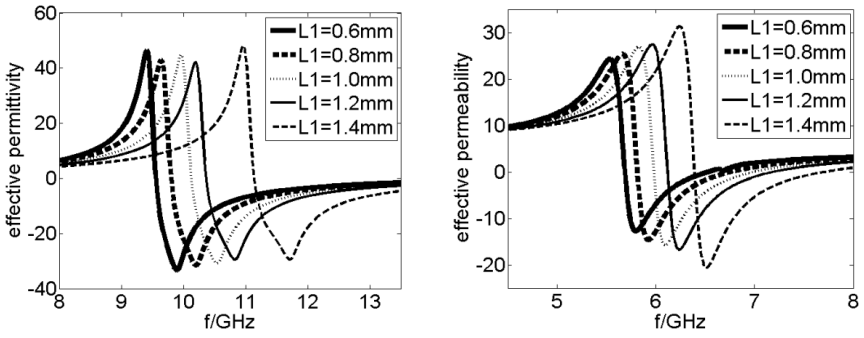

5(a) 5(b)

Figure 5. The Retrieved Parameter Versus Frequency Plot

(a) effective permittivity versus frequency plot; (b) effective permeability versus frequency plot

In Figure 3, it can be found that the wider of the X-direction width, the bigger the resonance frequency and the plasma frequency, as well as the regular of the X_1.

The parameter W_1 represents for the width of the Y-direction strip, and it varied in five steps of 0.2mm each, that is $W_1 = 0.6mm$, $W_1 = 0.8mm$, $W_1 = 1.0mm$, $W_1 = 1.2mm$, $W_1 = 1.4mm$.The effect of the X-direction distance on the effective permittivity and the effective permeability are shown in Figure 6 (a) and Figure 6 (b).

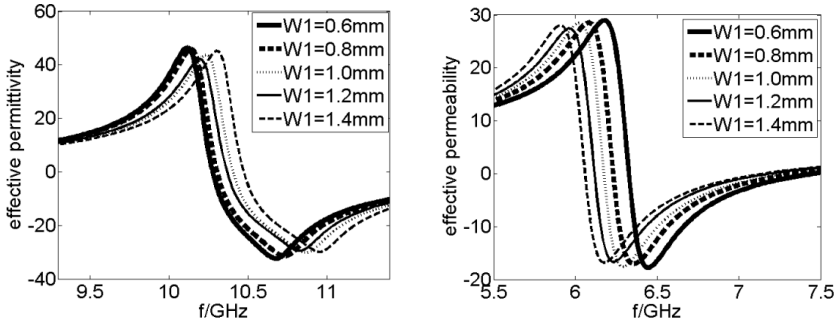

6(a) 6(b)

Figure 6. The Retrieved Parameter Versus Frequency Plot

(a) effective permittivity versus frequency plot; (b) effective permeability versus frequency plot

Figure 6 (a) shows that with the width increase, the negative frequency band of the effective permittivity shift from low frequency band to high frequency band. On the contrary, the negative frequency band of the effective permeability shift from high frequency band to low frequency band, as shown in Figure 6 (b). According to the equivalent circuit theory, the inductor is associated with the width of the Y-direction strip. With the width increase, the inductance decrease. Due to the inductance decrease, the magnetic resonance weaken. While the capacitance increased for the increase of the width, which leads to the enhance of the electric resonance. As a result, the negative frequency band of the effective permittivity shift from low frequency band to high frequency band, while the negative frequency band of the effective permeability shift from high frequency band to low frequency band.

The parameter t is used to represent for the thickness of the DSR. The thickness is varied in five steps for respectively 0.6mm, 0.8mm, 1.0mm, 1.2mm, and 1.4mm. The effect

on the effective permittivity and the effective permeability are demonstrated in Figure 7 (a) and Figure 7 (b).

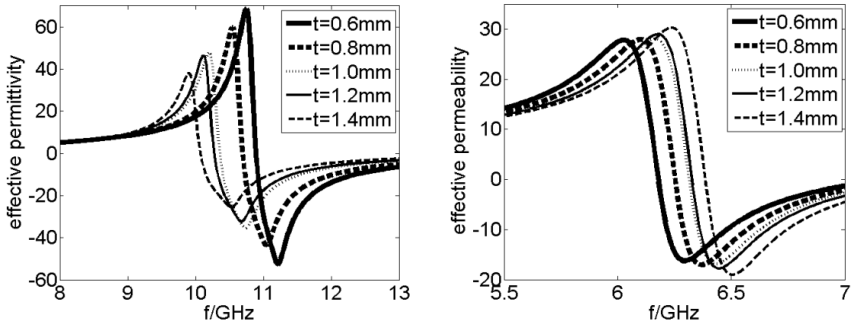

7(a) 7(b)

Figure 7. The Retrieved Parameter Versus Frequency Plot

a) effective permittivity versus frequency plot; (b) effective permeability versus frequency plot

The effect of the thickness is similar to the effect of the width of the Y-direction strip. As the thickness increase, the electric resonance weaken, while the magnetic resonance enhance.

With the distance from the square ring to the edge of the dielectric substrate decreased the length of the metallic strips increase. Therefore, the study of the parameter X_1 and the study of the parameter Y_1 are equivalent to the study of the length of the metallic strips.

The optimal structure is designed according to the results of the analysis above. The values of the parameters are included in Table 1, and the schematic is demonstrated in Figure 8(a). The effective permittivity and the effective permeability of the optimal structure are demonstrated in Figure 8 (b) and Figure 8 (c).

Figure 8 (b) and Figure 8(c) show that the effective permittivity is negative from 4.8GHz to 7.7GHz and the effective permeability is negative from 4.75GHz to 5.65GHz. Therefore, the frequency band of double negative extends from 4.8GHz to 5.65GHz.

Table 1. The Parameters of the DSR

Structural parameters	value
W0	10mm
L0	10mm
X1	0.2mm
Y1	0.2mm
W1	0.2mm
L1	1mm
t	0.4mm

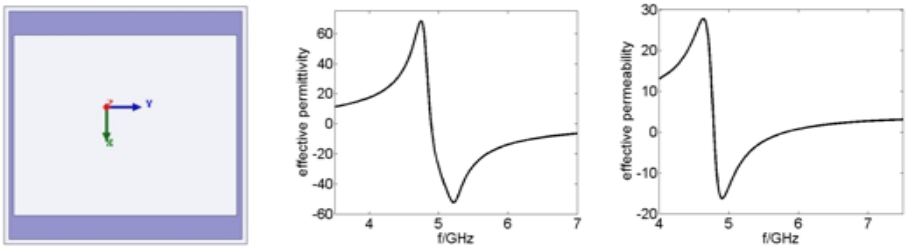

8(a) 8(b) 8(c)

Figure 8. The Retrieved Parameter of the DSR

(a) the schematic of the DSR(b) effective permittivity; (c) effective permeability

3. Microstrip Antenna Design

Table 2. The Parameters of the Conventional Microstrip Antenna

Structural parameters	value
L_s	36mm
W_s	32mm
L_p	16.4mm
W_p	12.4mm
t_s	2mm

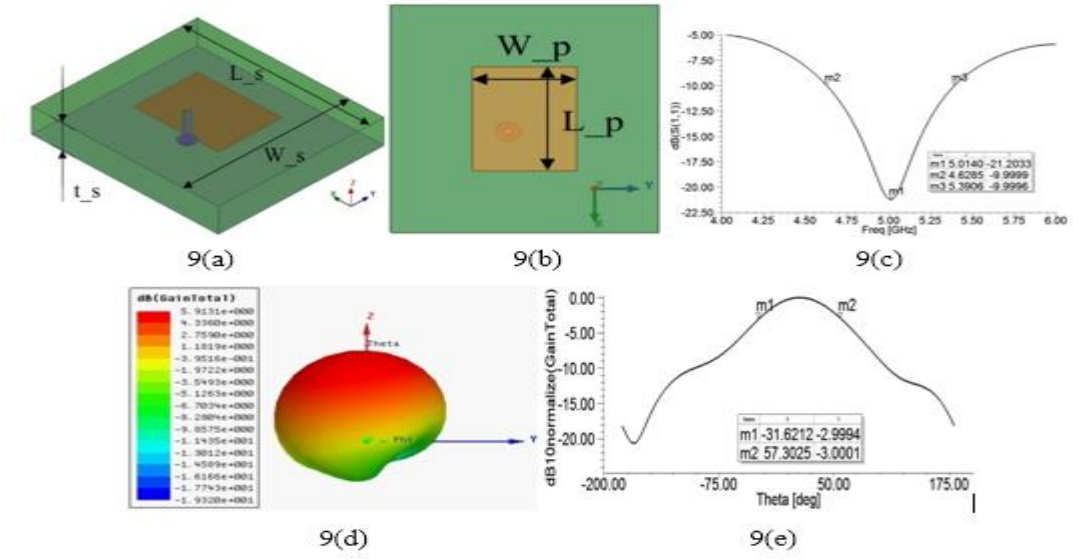

9(a) 9(b) 9(c)

9(d) 9(e)

Figure 9. The Performance of the Conventional Microstrip Patch Antenna

(a) angular view; (b) front view; (c) return loss; (d) gain; (e) HPBW

Microstrip patch antenna can be designed according to the empirical formula [14], and they are not written here for brevity. The values of each parameter are obtained as the result of the analysis of the parameters, as shown in Table 2.

The configuration of the microstrip patch antenna is demonstrated in Figure 9 (a) and Figure 9 (b). The size of antenna is $36\times32mm^2$, and the size of the patch is $16.4\times12.4mm^2$. The relative dielectric constant of the substrate is 4.4, and the height of the substrate is 2mm. The antenna is fed by the coaxial feed, and the antenna is designed at 50 Ω matching impedance. The simulation of the antenna is operated with the use of the HFSS software.

The return loss of the antenna is demonstrated in Figure 5(a), and the radiation pattern of the resonating frequency is shown in Figure 5(b), the half power beam width (HPBW) is demonstrated in Figure 5(c).

It shows that the resonating frequency of the antenna is 5.01GHz with the maximum return loss is -21.2dB, and the bandwidth is 770MHz. The gain of the antenna is 5.9dB with the HPBW is 88.9°.

4. High Gain Microstrip Antenna with Metamaterials

On the basis of the unit cell described in section Ⅱ, a single layered planar superstrate is designed. The superstrate is consist of the slab and the DSR array, the DSRs are constructed to form a 4×4 array and located at the top of the FR4 slab, as shown in Figure 10(a). The proposed antenna is consisting of the superstrate and the conventional microstrip patch antenna, as demonstrated in Figure 10(b).

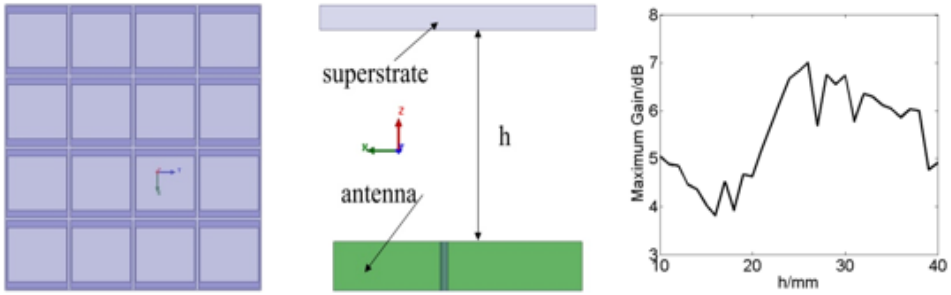

10(a) 10(b) 10(c)

Figure 10. The Schematic of the of the Novel Antenna

(a) front view of the superstrate; (b) side-view of the novel antenna; (c) the effect of the h on the gain;

The parameter h represents for the distance between the superstrate and the antenna, and the superstrate is in the antenna above. The distance between antenna and superstrate is varied in forty steps of 1mm each. At each step, a radiation characteristic is performed. To illustrate the effect of the distance on the maximum gain, Figure 10(c) is constructed.

Figure 10(c) shows that the maximum gain of the proposed antennas is 7.01dB when the h is 26mm. The longer the distance between antenna and superstrate, the higher the maximum gain of the antenna. However, as the distance more than a certain degree, the maximum gain of the antenna is decreased.

It found that the direction of the radiation reversed when the distance small. The radiation pattern when the distance is 3mm is shown in Figure 11 (c), the radiation pattern of the conventional microstrip antenna and the radiation pattern when the distance is 26mm are demonstrated as comparison. It is clear that the direction of the radiation reversed when the distance is 3mm, and this case also appeared in other condition with small distance. When the distance close to the half-wavelength, the electromagnetic wave can be converged by the superstrate [14], as shown in Figure 11 (b).

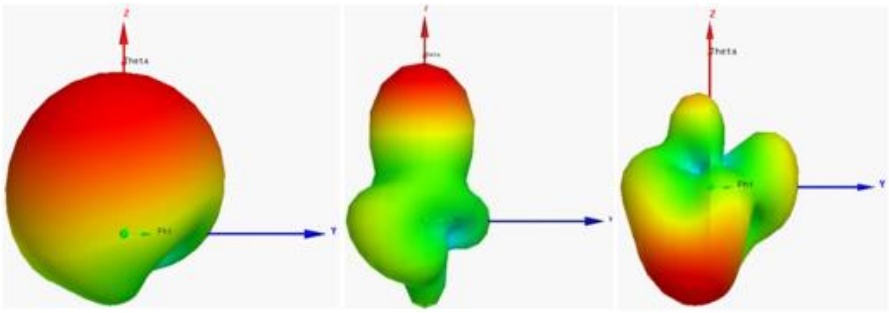

11(a) 11(b) 11(c)

Figure 11. The Radiation Pattern in Three Cases

(a) conventional microstrip antenna; (b) h=26mm; (c) h=3mm;

After the analysis of the distance between the superstrate and the antenna, the best result is used for the novel antenna. The novel antenna has the distance of 26mm between the antenna and the superstrate. The return loss of the novel antenna is shown in Figure 12(a), and the radiation pattern is demonstrated in Figure 12 (b), the HPBW is shown in Figure 12 (c).

It shows that the resonating frequency of the novel antenna is 4.99GHz, almost consistent with the microstrip antenna designed in section Ⅲ. The gain of the novel antenna is 7.01dB. The HPBW of the novel antenna is 48°, while the designed conventional microstrip antenna's HPBW is 88.9°, decreased by 40.9°.

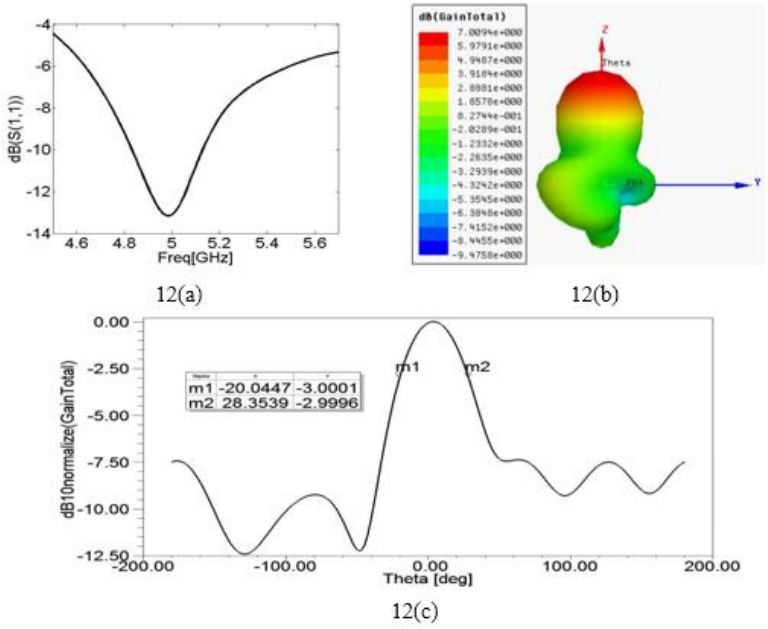

Figure 12. The Performance of the Novel Antenna

(a) return Loss; (b) gain; (C) HPBW

5. Conclusion

In this paper, the conventional DSR metamaterial is proposed at first. The distribution of the electromagnetic field of the conventional DSR is analyzed to deduce the equivalent circuit of the conventional DSR. According to the equivalent circuit theory, the effect of the structural parameters on the effective permittivity and the effective permeability are proposed. It is found that the structural parameters have an effect on the effective

permittivity and the effective permeability. The novel DSR metamaterial is designed based on the analysis of the structural parameters, the effective permittivity and the effective permeability of the novel DSR are negative within the scope of the 4.8GHz to 5.65GHz. The designed conventional microstrip antenna is proposed based on the empirical formula, and its maximum gain is 5.9dB at 5.01GHz. The novel antenna is consist of the conventional microstrip antenna and the superstrate, and the superstrate is constructed by the DSR metamaterials. The distance between the conventional microstrip antenna and the superstrate has an effect on the gain of the novel antenna. As a result of the analysis of the distance, it is found that the direction of the radiation reversed when the distance less than a quarter wavelength, and the electromagnetic wave can be converged by the superstrate when the distance is half-wavelength. The simulation results show that the novel antenna's maximum gain is 7.01dB at 4.99GHz, improved by 1.01dB. The novel antenna's HPBW is 48°, decreased by 40.9°.The novel DSR metamaterial structure proposed in this paper provides a reference for the design and practical applications of metamaterials in the future.

References

[1] H. X. Liu, L. Shuo, X. W. Shi and L. Li, "Study of antenna superstrates using metamaterials for directivity enhancement based on fabry-perot resonant cavity", Int. J. Antenn. Propag. 209741, **(2013)**.
[2] D. D. Yavuz, N. R. Brewer. Left-handed electromagnetic waves in materials with induced polarization and magnetization. Rhys. Rev. A., no. 90, **(2014)**.
[3] A. Sharma, S. K. Gupta, B. K. Kanaujia, G. P. Pandey and M. Sharma, "Design and analysis of a meandered multiband antenna based on split ring resonator", Microw. Opt Techn. Lett., vol. 55, no. 11 **(2013)**.
[4] Z. L. Ma, L. J. Jiang, S. Gupta and W. E. I. Sha, "Dispersion characteristics analysis of one dimensional multiple periodic structures and their applications to antennas", IEEE T. Antenn. Propag., vol. 63 no. 1 **(2015)**.
[5] H. S. Zhong, P. Yin and R. X. Wu, "An implementation of directional antenna by self-biased magnetic photonic crystal", Appl. Phys. A, vol. 117, **(2014)**.
[6] D. R. Smith and N. Kroll, "Negative Refractive Index in LHMs. Phys. Rev. Lett., vol. 85, no. 14, **(2000)**.
[7] D. R. Smith, D. C. Vier, N. Kroll and S. Schultz. Direct calculation of permeability and permittivity for a left-handed metamaterial. Appl. Phys. Lett., vol. 77, no. 14, **(2000)**.
[8] Y. Shen and L. L. Gong, "Investigation of gain effect of multi-band patch antenna based on composite rectangular SRRs",Optik, vol. 125, **(2014)**.
[9] S. Mondal and P. P. Sarkar, "Design of an extremely wideband planar elliptical metal antenna. IEEE. Antennas Wireless Rropag. Lett., vol. 12, **(2013)**.
[10] A. Belenguer, A. L. Borja and V. E. Boria, "Balanced dual composite rightleft-handed microstrip line with modified complementary split-ring resonators", IEEE. Antennas Wireless Rropag. Lett., vol. 12 **(2013)**.
[11] K. S. Zheng, N. J. Li, A. K. Ren, G. Wei and J. D. Xu, "Designing and measurement of a single layered planar gain-enhanced antenna radome with Metamaterials", J. of Electromagn. Waves and Appl., vol. 26, **(2012)**.
[12] P. Katiyar and W. N. L. W. Mahadi, "Impact analysis on distance variation between patch antenna and metamaterial", Microw. Opt Techn. Lett., vol. 57, no. 1, **(2015)**.
[13] W. B. Pan, C. Huang, P. Chen, X. L. Ma, C. G. Hu and X. G. Luo, "A low-rcs and high-gain partially reflecting surface antenna", IEEE T. Antenn. Propag., vol. 62, no. 2, **(2014)**.
[14] L. Y. Guo, H. L. Yang, M. H. Li, C. S. Gao and Y. Tian, "A mircostrip antenna with single square ring structured left-handed metamaterial", Acta. Phys. Sin,vol. 61, no. 1, **(2012)**.
[15] D. R. Smith, W. J. Padilla, D. C. Vier, S. C. Nemat-Nasser and S. Schultz, "Composite medium with simultaneously negative permeability and permittivity", Phys. Rev. Lett., vol. 84, no. 18, **(2000)**.
[16] H. S. Chen, L. X. Ran, J. T. Huangfu, X. M. Zhang and K. S. Chen, "Left-handed materials composed of only S-shaped resonators", Rhys. Rev. E., vol. 70, **(2004)**.
[17] J. P. Turpin, J. A. Bossard, K. L. Morgan, D. H. Werner and P. L. Werner, "Reconfigurable and tunable metamaterials a review of the theory and applications", Int. J. Antenn. Propag., no. 429837, **(2014)**.
[18] P. Gao, C. M. Zhang, J. J. Ai, G. Li and Y. Q. Kang, "Measurement of negative refraction index from simulative results and experimental data by a new metamaterial sample", Physica A., no. 392, **(2013)**.
[19] J. F. Wu, "The thickness of substrate influence on the resonant frequency in the LHMs", Optik, no. 124, **(2013)**.

Authors

Tong Huang (1980.6), male, Nanyang City of Henan Province, China, lecturer, graduate. Research areas: communication system, modern signal processing, underlying driver development, DSP embedded system design *etc*. Once, worked in GE China engaged in OA software development based on Lotus Domino/Notes, in China National Software and Service Co., Ltd for system software development, in Huawei for driven research and development of WCDMA standards 3G Mobile terminal. Now engaged in signal processing research and related courses teaching as primary lecturer in XIAN Innovation College of YANAN University.